Energy radiation of moving cracks

S. Fratini,[1] O. Pla,[1] P. González,[2] F. Guinea,[1] and E. Louis[3]
[1]*Instituto de Ciencia de Materiales, Consejo Superior de Investigaciones Científicas, Cantoblanco, E-28049 Madrid, Spain*
[2]*Departamento de Física, Universidad Carlos III, Butarque 15, Leganés, 28913 Madrid, Spain*
[3]*Departamento de Física Aplicada, Universidad de Alicante, Apartado 99, E-03080 Alicante, Spain*
(Received 22 October 2001; revised manuscript received 28 February 2002; published 17 September 2002)

The energy radiated by moving cracks in a discrete background is analyzed. The energy flow through a given surface is expressed in terms of a generalized Poynting vector. The velocity of the crack is determined by the radiation by the crack tip. The radiation becomes more isotropic as the crack velocity approaches the instability threshold.

DOI: 10.1103/PhysRevB.66.104104 PACS number(s): 62.20.Mk, 65.40.De

I. INTRODUCTION

The dynamics of cracks in brittle materials are being extensively studied,[1,2] and a wealth of instabilities and patterns have been observed as a function of control parameters such as the applied strain,[3–7] or thermal gradients.[8] The theoretical analysis of moving cracks was initiated long ago,[9–11] with the study of exact solutions for cracks moving at constant velocity. These studies have been extended to a variety of different situations.[12,13] Alternatively, analytical approximations to the leading instabilities of a moving tip have been proposed.[14]

The simplest discrete model that captures the main features of cracks in brittle materials is a lattice with central forces (springs) between nearest neighbors, whose bonds lose the restoring force above a given threshold[15] (for extensions see also Ref. 16). This model, or simplifications of it which leave out the vectorial nature of the strain field, has been extensively used in modeling moving cracks,[2,13,17–19] although models that deal with the microscopic structure of the system are also being considered.[20–23] Alternatively, various continuum models, which describe the fractured zone in terms of additional fields, have been proposed.[24,25]

Discrete and continuum models of cracks differ in a variety of features. It is known that the discrete models used so far cannot describe a fracture zone at scales other than the size of the lattice cell in the calculations,[18,26] although, even for a canonical material such as polymethylmethacrylate (PMMA), the fracture zone has a dimension much larger than the size of its molecular building blocks.[27]

Another important difference between discrete and continuum models is the existence of radiation from the tip of the moving crack, due to the existence of periodic modulations in the velocity in the presence of an underlying lattice. In this sense, a lattice model for cracks is the simplest example where radiation due to the scattering of elastic waves by deviations from perfect homogeneity can be studied. These processes have been observed in experiments,[6,28–30] and it has been argued that these are responsible for some of the crack instabilities.[30]

In the present work, we study the energy radiated by a crack moving at constant velocity in a discrete lattice. We use a generalization of the scheme discussed in Ref. 1. The general method used is explained next. Section III presents the main features of the results. The physical implications of the results are discussed in Sec. IV.

The problem of sound emission by moving cracks has been addressed, within a different scheme in Ref. 31. Insofar as the two approaches can be compared, the results are compatible. Finally, radiation of moving cracks along the edge of the crack can be important in understanding the roughness of the crack surface.[32] We will focus on the radiation along the crack surface, and into the bulk of the sample. Experiments[30] and simulations[2] suggest that this type of radiation can play a role in the observed instabilities of the crack tip.

Absorption of the sound waves emitted from the crack can lead to significant heating of the region around the crack tip, which may help to explain some experimental results.[33] In the present work we are not considering the detailed interplay between dissipation, heating effects, and crack morphology.[34] It will be interesting to have more experimental information available, especially in materials with high dissipation, such as PMMA.

II. THE METHOD

We study discrete models of elastic lattices in two-dimensional stripes, as discussed in (Ref. 17 and 18). The underlying lattice is hexagonal, with nearest-neighbor forces. Bonds break when their elongation exceeds a given threshold, u_{th}, and under a constant strain at the edges, which, scaled to the width of the stripe, we denote as u_0. We study models with and without dissipation in the dynamics of the nodes. Results depend on the ratio u_{th}/u_0 (see Sec. III for further details).

A. Energy considerations

In the absence of dissipation, the total kinetic-plus-elastic energy must be conserved. In a continuum model, in the absence of radiation, energy conservation leads to a global and to a local constraint, for cracks moving at constant speed, v.

(i) In the absence of radiation, the region well behind the crack tip has relaxed to equilibrium, while the region ahead of it is under the applied strain. The relaxed region grows at the expense of the region under strain, at constant rate $\propto u_0^2 v W$ where W is the width of the stripe.[18] Energy is trans-

ferred to the crack at this rate. As the energy stored in the crack grows at rate $\propto u_{th}^2 v$, the crack can only propagate (without radiation) for a fixed value of u_{th}/u_0. Note that continuum solutions for radiationless cracks moving at constant speed[9] do not specify a parameter equivalent to u_{th}, so that they do not conflict with energy conservation.

(ii) It is commonly assumed that the dynamics of the crack is determined by the energy flow at the crack tip,[1,35] which is the only region where new crack surfaces are created. In continuum models, this local constraint leads to an equation of the type

$$\Gamma = A(v)G, \tag{1}$$

where Γ is the crack energy per unit length ($\Gamma \propto u_{th}^2$ in our lattice model), G is proportional to the stress intensity factor at the crack tip, and $A(v)$ is a universal function that goes from 1 at $v=0$ to 0 at $v=v_R$ where v_R is the Rayleigh speed.

In the absence of radiation from the crack tip, both constraints can only be satisfied at a given velocity, such that the energy flux invested in enlarging the crack, $A(v)G$ in Eq. (1), balances the loss of elastic energy throughout the lattice.

Simple scalar models, such as those describing the propagation of type-I cracks in a continuum, can be obtained by a Lorentz transformation from static solutions. When this is the case, the crack cannot radiate. A type-III crack in a finite slab can couple to a particular transverse model, even in the continuum limit (see the Appendix). In the this case, and in the absence of a short-distance cutoff, the single mode that can be excited by a crack moving at a constant speed has null measure. Hence, its contribution to the radiation is negligible. In the presence of a short-distance cutoff, a, we expect the energy radiated by this mode to decay as a power law, $d\epsilon/dt \propto (a/l)^{\alpha}$, where l is the width of the slab, and $\alpha \geqslant 1$ is a constant.

In lattice models, the energy arguments discussed earlier have to be modified because of the presence of radiation of elastic waves at wavelengths comparable to the lattice spacing. If we assume that the difference between continuum and lattice models is small, we can use the perturbative scheme discussed in Refs. 36–40. The crack tip velocity undergoes oscillations at frequency $\omega = v/a$, where a is the lattice constant, and amplitude $f(v)$. In order to estimate the energy radiated from the tip, we have to extend the perturbative expansion to second order. We will not attempt here to calculate this expansion rigorously. However, from the knowledge of the leading term,[38,40] we can infer that the radiation due to a perturbation of frequency ω should go as $B\omega^2$, where B is a positive constant. Hence, the power radiated by the crack when it moves goes as $f(v)^2 (v/a)^2$.

The existence of radiation modifies the global- and local-energy constraints described above. The energy in regions far from the crack is not purely elastic, and it has a kinetic contribution. In addition, the energy flux at the crack tip acquires an additional velocity dependence. Thus, radiation in discrete models allows for the existence of a continuum of solutions, $v(u_0/u_{th})$ $v(u_0/u_{th})$.[12,13,17–19]

Note that the existence of solutions that do not violate energy conservation does not imply that these solutions are stable. Full dynamical simulations of lattice models[17–19] suggest that inertial cracks (without dissipation) accelerate until they reach speeds comparable to those predicted by the Yoffe criterion,[9] and then bifurcate.

The above considerations about the balance of elastic energy, radiation, and crack formation energy in continuum and lattice models can be extended to more realistic situations, such as those being analyzed experimentally. In principle, if the crack formation energy is independent of velocity, which is probably a good approximation if the morphology of the crack does not change much, some of the crack energy has to be radiated by the tip. Otherwise, cracks will only move at constant velocity for a particular value of the applied strain. The radiation from the tip, however, will be mostly determined by the scattering of the crack tip from random defects that modify locally the elastic properties of the material. The radiation emitted will not show preferred frequencies, as in the lattice model considered here.

B. Energy flux: Continuum elasticity

In the following, we will reformulate the concepts discussed in Ref. 1 in order to make them more amenable for extensions to lattice models, dicussed in Sec. II C.

We describe an elastic medium in terms of the energy,[41]

$$\mathcal{H} = \mathcal{H}_{kin} + \mathcal{H}_{elastic},$$

$$\mathcal{H}_{kin} = \int d^D r \frac{\rho}{2} \left(\frac{\partial \mathbf{u}(\mathbf{r})}{\partial t} \right)^2, \tag{2}$$

$$\mathcal{H}_{elastic} = \int d^D r \frac{\lambda}{2} \left(\sum_i u_{ii} \right)^2 + \mu \int d^D r \sum_{ij} u_{ij}^2,$$

where D is the spatial dimension, ρ is the mass density, λ and μ are Lamé coefficients, $\mathbf{u}\cdot(\mathbf{r})$ denotes the displacements at position $\mathbf{r}$, and the u_{ij}'s define the strain tensor

$$u_{ij}(\mathbf{r}) = \frac{1}{2} \left(\frac{\partial u_i}{\partial r_j} + \frac{\partial u_j}{\partial r_i} \right). \tag{3}$$

The equations of motion satisfied by $\mathbf{u}\cdot(\mathbf{r})$ can be written as

$$\rho \frac{\partial^2 u_i}{\partial t^2} = -\sum_j \frac{\partial}{\partial r_j} \sigma_{ji}, \tag{4}$$

where $\sigma_{ji} = \partial \mathcal{H}_{elastic} / \partial u_{ij}$ is the stress tensor.

The time derivative of the total energy E_Ω within a region Ω is

$$\frac{\partial E_\Omega}{\partial t} = \frac{\partial}{\partial t}\int_\Omega d^D r[\mathcal{H}_{kin}+\mathcal{H}_{elastic}]$$

$$= \int_\Omega d^D r\left[\rho\frac{\partial \mathbf{u}}{\partial t}\frac{\partial^2 \mathbf{u}}{\partial t^2}+\frac{\partial u_{ij}}{\partial t}\sigma_{ij}\right]$$

$$= -\int_\Omega d^D r\frac{\partial}{\partial r_j}\left(\sigma_{ij}\frac{\partial u_i}{\partial t}\right), \quad (5)$$

so that the vector $\mathbf{P}\cdot(\mathbf{r})$ with components $P_j=\Sigma_i\sigma_{ij}\partial u_i/\partial t$ plays the same role as the Poynting vector in electrodynamics. The energy flux through an element of area $d\mathbf{S}$ is given by $\mathbf{P}d\mathbf{S}$. Note, however, that, unlike in electromagnetism, the equations of elasticity have no Lorentz invariance (there are two sound velocities), and it is not possible to define a four-vector combining **P** and the energy density. The energy transferred to the outside of this region remains defined as the flux of the vector **P** through the surface bounding Ω. In the presence of dissipation, we still use **P** as defined in Eq. (5) in the understanding that what viscosity does is to trigger the partial absorbtion of the radiated energy without changing the direction in which it is emitted. The vector **P** will be our starting point in the study of the energy flux of a moving crack.

C. Energy flux: Lattice model

We will compute numerically the radiation of energy in a discrete model, defined as a hexagonal two-dimensional lattice with nearest-neighbor forces.[15,17,18] The energy is given by the sum of a kinetic term, associated to the velocities of the nodes, and an elastic term, due to the deformation of the bonds. The variation of the elastic energy of a given bond with time can be written as

$$\frac{\partial E_{ij}}{\partial t} = k[(\mathbf{u}_i-\mathbf{u}_j)\mathbf{n}_{ij}]\frac{\partial[(\mathbf{u}_i-\mathbf{u}_j)\mathbf{n}_{ij}]}{\partial t}, \quad (6)$$

where k is the force constant, and $\mathbf{n}_{ij}$ is a unit vector in the direction of the bond. We distribute this energy among the two nodes connected by the bond, so that we can write the total elastic energy within a given region as a sum of the contributions of the nodes within that region. As in the continuum limit, we can use the equations of motion to estimate the variation in the kinetic energy at node i, which can be written as

$$\frac{\partial K_i}{\partial t} = -k\sum_j \frac{\partial(\mathbf{u}_i\cdot\mathbf{n}_{ij})}{\partial t}[(\mathbf{u}_i-\mathbf{u}_j)\mathbf{n}_{ij}]. \quad (7)$$

The variation of the total energy within a given region is calculated by summing over all bonds within that region. The kinetic and elastic contributions for all bonds outside the edge of the region cancel. We are left with surface terms only, as in the continuum model described earlier. The surface contributions can be written as a sum of terms associated to the bonds that connect a node within the region under study and a node outside. Thus, a surface that includes a given node and has a given orientation leads to an energy flux across it, which can be calculated from a weighted sum of the positions and velocities of the bonds that connect that node to its neighbors. As we can associate to each surface orientation an energy flux, we can define the lattice Poynting vector, in analogy to the analysis done for the continuum model. We will use this discrete Poynting vector in the discussion of the energy dissipation of a moving crack below.

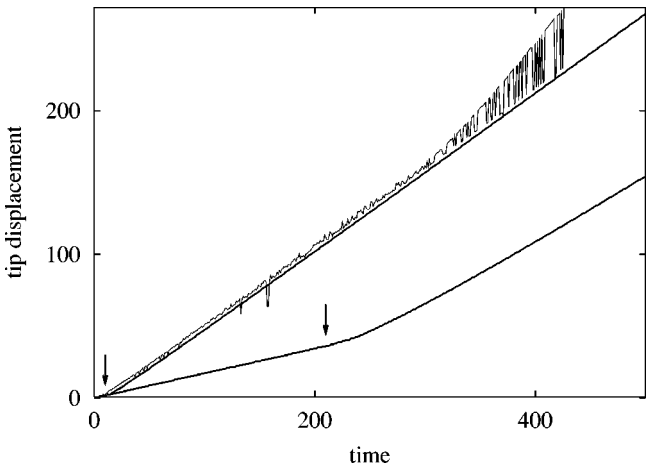

FIG. 1. Crack velocity versus time for cracks under two different applied strains and zero viscosity. The arrow indicates the position of the notch beyond which the stresses at the crack tip exceed the threshold stress, and the crack propagates freely.

III. RESULTS

The discrete equations of motion in a two-dimensional lattice of a given size are integrated numerically as discussed in detail elsewhere.[18] The lattice is maintained under constant load at the edges. In order to obtain cracks moving at constant velocities, a notch is induced at one side, which is gradually enlarged, along a straight line, until the stress buildup leads to the spontaneous propagation of the crack. The crack position, as a function of time, is shown in Fig. 1

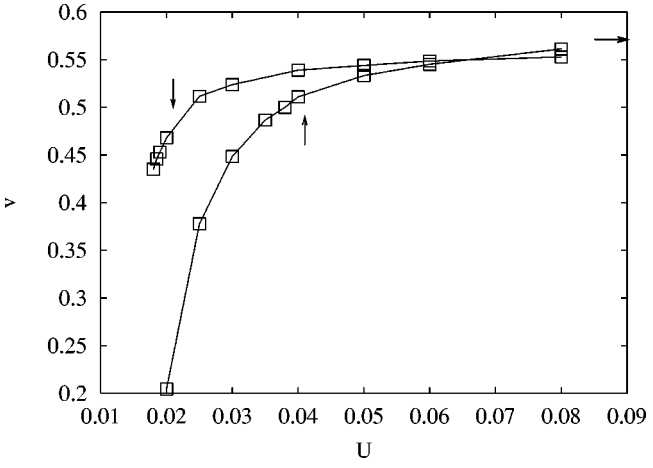

FIG. 2. Crack velocity versus external strain, for $\eta=0$ (upper curve) and $\eta=0.8$ (lower curve). The arrow on the right indicates the Rayleigh velocity v_R. The vertical arrows mark the (avoided) branching instability (see text). The threshold for breaking is $u_{th}=0.1$.

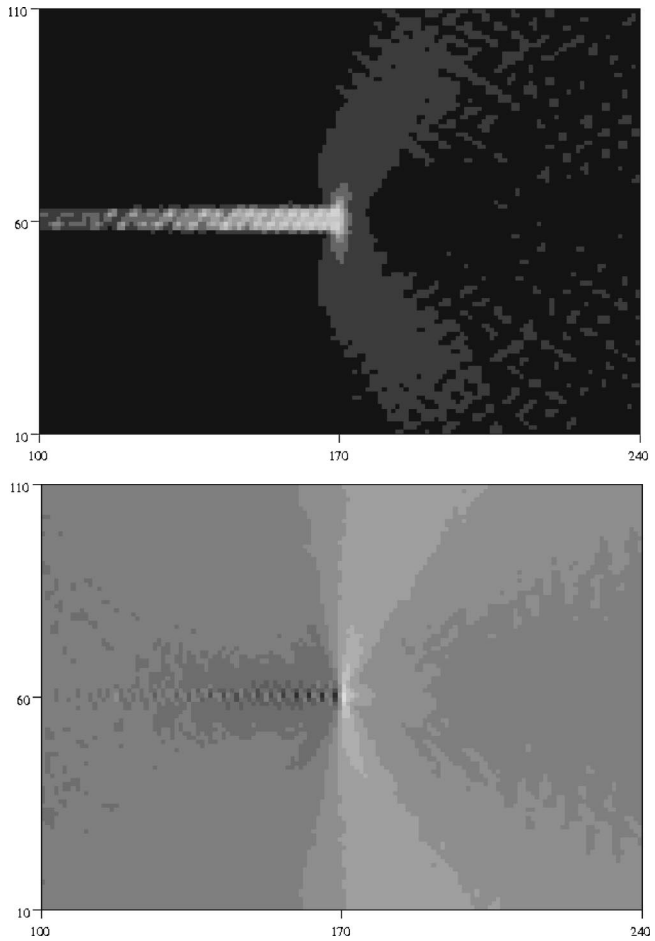

FIG. 3. Density of elastic energy (upper panel) and hoop stress (lower panel) for an inertial crack ($\eta=0$) moving under an applied strain $u_0=0.02$, below the branching instability. The crack moves from left to right, and the tip is located at the point of coordinates 170,60.

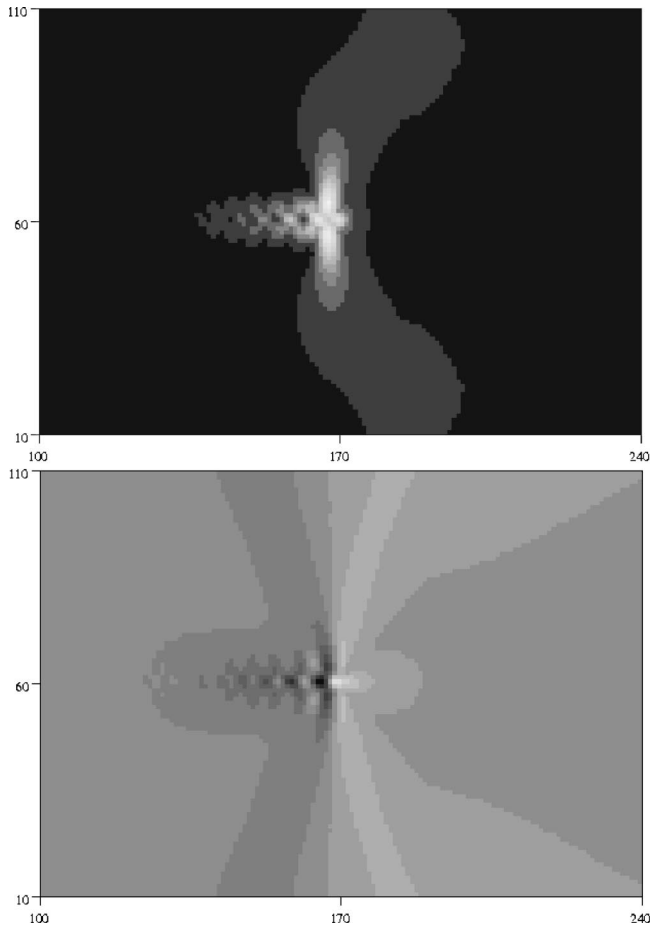

FIG. 4. Density of elastic energy (upper panel) and hoop stress (lower panel) for an inertial crack ($\eta=0$) moving under an applied strain $u_0=0.08$, well above the branching instability.

for two different applied strains. The calculations show that the crack propagates freely at a constant velocity in the steady state. Our method for the calculation of the properties of cracks moving at constant speeds should lead to the same results as given by other techniques.

Instabilities are avoided by allowing only the bonds directly ahead of the crack to break. In other words, we force the crack to propagate straight (with no branching). The simulations are performed in systems of 400×120 lattice sites, where we have checked that finite-size effects on the steady-state velocity are less than 1%.

A. Crack velocity

Figure 2 shows the steady-state velocity v as a function of the applied strain u_0, for two different values of the viscosity ($\eta=0$ and $\eta=0.8$ in our units). The crack velocity increases monotonically with u_0 and asymptotically tends to its limiting value $c_R=0.571$, the Rayleigh velocity in units where the force constant $k=1$ and the mass per site $m=1$.[16] Due to lattice trapping, there is a minimum allowed u_0 whose value is roughly independent of η,[13,42] which in turn leads to a minimum crack speed that depends strongly on η. The arrow marks the instability that would occur if the crack were not constrained to move on a straight line.

B. Elastic energy and hoop stress

Figure 3 shows snapshots of the density of elastic energy and the hoop stress at a given time t_0, for a steady inertial crack ($\eta=0$) moving at a velocity below the branching threshold (the applied strain is $u_0=0.02$, cf. Fig. 2).

The density of elastic energy (Fig. 3, upper panel) has a sharp peak at the crack tip. In the near region (a few lattice spacings away from the tip), we see that the distribution of elastic energy is very anisotropic: it is sizable in the direction perpendicular to the crack motion, where it decays smoothly with the distance, and all along the crack, where it has an oscillating behavior. This behavior is reminiscent of the Rayleigh waves that propagate on the crack surface (see Sec. III C below). At larger distances (of the order of the linear dimensions of the system), the elastic energy is smoother and has a broad maximum ahead of the tip, around a given angle of the order of $\theta\approx\pi/3$ from the crack direction. We cannot be conclusive about this maximum being intrinsic in nature,

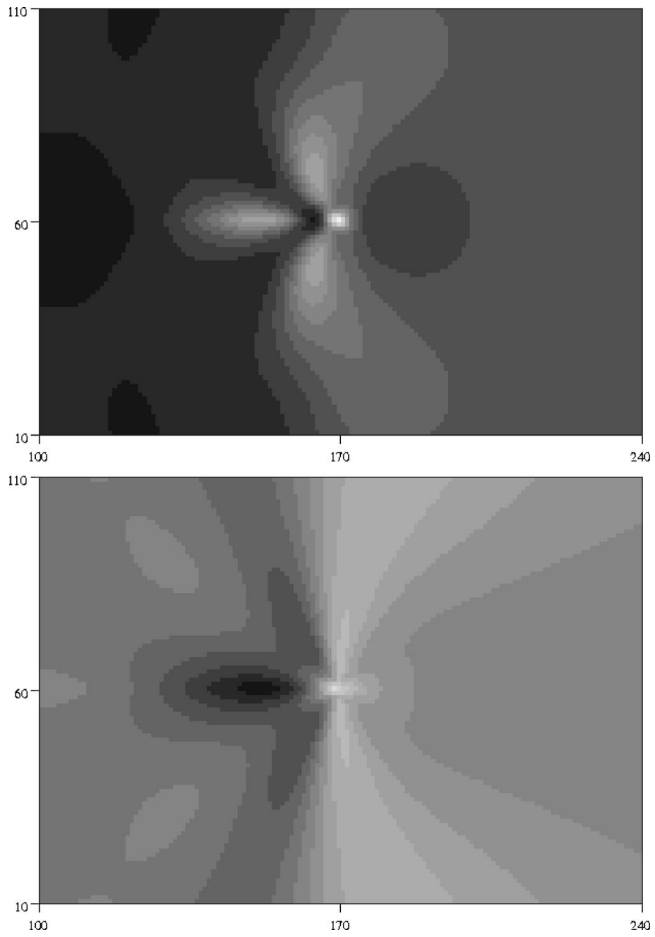

FIG. 5. Density of elastic energy (upper panel) and hoop stress (lower panel) for a dissipative crack ($\eta=0.8$) moving under an applied strain $u_0=0.08$.

or rather being related to the symmetry of the underlying triangular lattice (see Ref. 19 for a more detailed discussion of this point).

The hoop stress (Fig. 3, lower panel) shows a very similar behavior, with strong oscillations all along the crack, and maxima perpendicular to the crack motion, the maximum shifting from $\theta\approx\pi/2$ to $\theta\approx\pi/3$ with increasing distance from the tip.

Figure 4 is the same as Fig. 3, but for a crack moving at a velocity well above the branching threshold (the applied strain is $u_0=0.08$). We notice that the distribution of elastic energy and hoop stress has changed qualitatively: the bulk features in the direction perpendicular to the crack motion now dominate over the oscillating part along the crack. The latter decay more rapidly and eventually disappear far behind the tip.

The elastic energy and hoop stress corresponding to a *dissipative* crack ($\eta=0.8$, $u_0=0.08$) are shown in Fig. 5. Although the overall characteristics are similar to the inertial case, with maxima at the tip and in the direction transverse to the crack, the distribution of stresses is much smoother. Moreover, the oscillations associated with Rayleigh waves along the crack are washed out by viscosity, being replaced by a single broad maximum behind the tip.

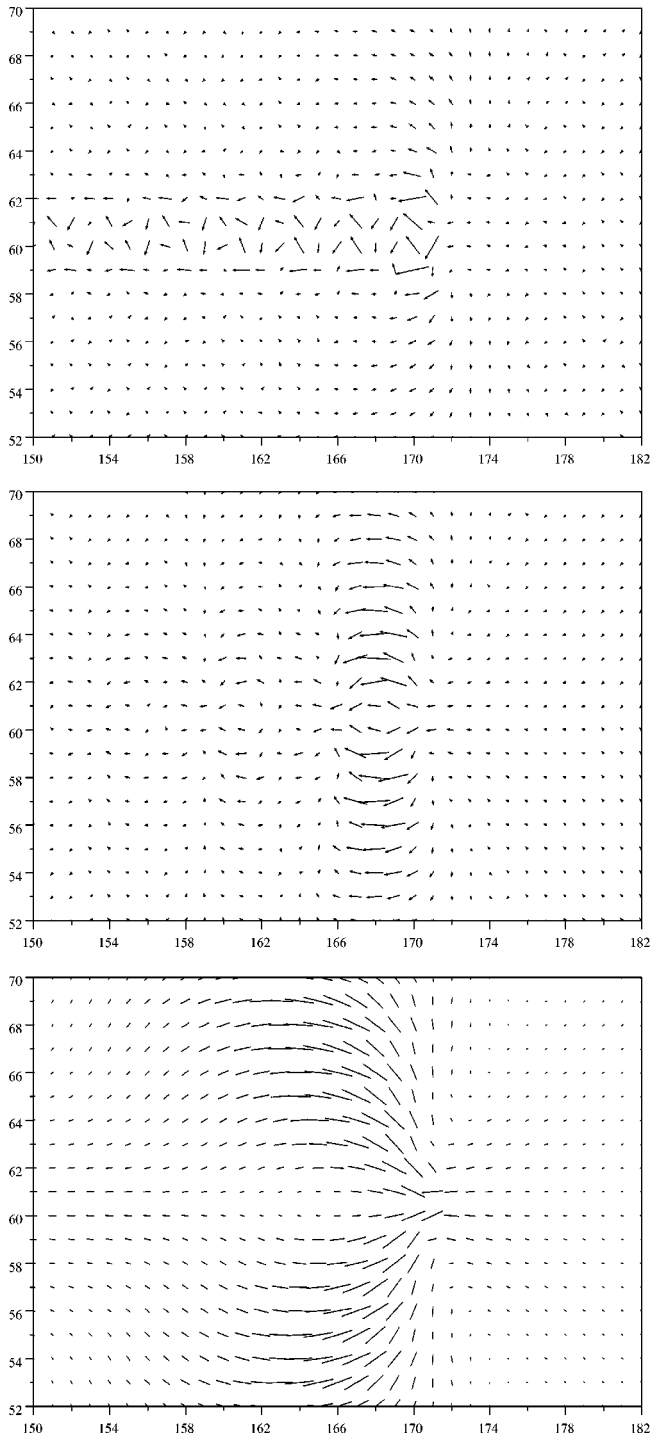

FIG. 6. Poynting vector field representing the radiation propagating in the vicinity of the crack tip. Upper panel, slow inertial crack (same parameters as in Fig. 3); center panel, fast inertial crack (same as Fig. 4); lower panel, dissipative crack (same as Fig. 5).

C. Radiation

The above results can be better understood by analyzing the Poynting vector field that represents the flux of energy being radiated at a given point in the system. As was stated in the Introduction, emission of sound waves is expected since the crack tip moves in a *discrete* medium, therefore acting as a source of radiation at a frequency $\nu=v/a$, the

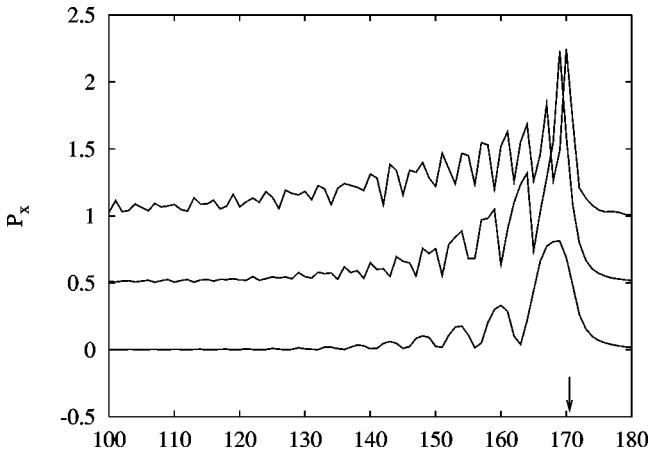

FIG. 7. The component of the Poynting vector along an inertial crack, as a function of the coordinate x, normalized to the total energy flowing through the sample, $\propto u_0^2 v W$ (see text). From top to bottom: $u_0 = 0.02$, 0.04, 0.08. The vertical arrow marks the tip position. The curves are shifted by a vertical offset for clarity purposes.

ratio of the crack speed to the lattice spacing. Moreover, one expects a net flux of energy in the direction *opposite* to the crack motion, corresponding to the elastic energy released from the region ahead of the tip, which allows the crack to move.

As can be seen in the first panel of Fig. 6, at such moderate crack speeds most of the energy is radiated in the form of Rayleigh waves propagating backwards along the crack, with a wavelength comparable with (but not equal to) the lattice spacing a. Despite the fact that $\eta = 0$, such waves are seen to decay at long distances behind the tip (they decay into bulk waves, the oscillating bonds on the crack surface acting themselves as sources of radiation. In addition, there is also a weaker emission of bulk waves from the tip, responsible for the observed maximum in the direction perpendicular to the crack motion.

At high crack speeds, on the other hand (cf. center panel in Fig. 6), it is the bulk radiation that dominates the emission pattern. Moreover, shadow images of the near-field appear behind the tip (the strongest one being at around $x = 161$), which can arise.

In the case of viscous cracks (lower panel in Fig. 6), the emission pattern is entirely dominated by bulk waves, and Rayleigh oscillations disappear as suggested by the results of Fig. 5.

In order to analyze the behavior of Rayleigh waves along inertial cracks, we plot in Fig. 7 the component of the Poynting vector P_x parallel to the crack direction, at the surface of the crack, for different values of the applied strain. The data are normalized to the difference in the mechanical energy of a line far ahead from the crack, and a line far behind (this energy, which scales as $u_0^2 v W$, is transferred to the crack in the fracture process). The figure clearly shows that the wavelength of surface waves as well as their decay rate increase with the crack velocity.

IV. CONCLUSIONS

We have analyzed the nature and influence of radiation in the propagation of cracks in discrete systems. For the lattice and force models that we have studied, we make the following remarks.

(i) Cracks in lattice models radiate energy at wavelengths comparable to the lattice spacing, even when the average velocity is constant and the cracks move along a straight line. This can be understood by assuming that the crack tip undergoes oscillations at frequencies nv/a, where v is the velocity of the crack and a is the lattice constant.

(ii) Radiation allows for the existence of a continuum of solutions of moving cracks at constant velocity. The balance of static elastic and crack energy is compensated by the radiation from the crack tip.

(iii) At low velocities, most of the radiation is in Rayleigh waves along the surface of the crack. At velocities comparable to the Rayleigh velocity, a significant fraction of the radiated energy is in bulk waves with a more isotropic distribution.

(iv) Viscosity allows for a faster exchange of the elastic energy stored ahead of the crack tip into other forms of energy. This can help to explain the increased stability of straight cracks in the presence of viscosity.

Among the questions that remain unsolved is the relation of the radiation to the instabilities of the crack tip. Our results suggest that inertial cracks accelerate along a straight line, until they attain speeds compatible with Yoffe's criterion.[9] On the other hand, the radiation of the crack tip becomes more isotropic at high velocities. It is unclear whether the continuum approach suffices to understand the instability observed in dynamical simulations of discrete models, or if the radiation from the tip of the crack plays a role in the instability. Note that the calculated instability occurs at higher velocities than the instabilities observed experimentally.

Finally, the radiation considered here arises from the modulation of the velocity of the crack tip that arises from the existence of a discrete lattice. In typical experimental situations, the variations in the velocity of the crack will be most likely due to random scatterers that modify locally the elastic properties of the system. Hence, the radiation will not have preferred frequencies, as in the present case, and will probably show up as random acoustic noise. The power spectrum of this noise, as a function of the crack velocity can be an interesting topic to study, both theoretically and experimentally.

ACKNOWLEDGMENTS

We are thankful to R. Ball, P. Español, M. Marder, T. Martín, A. Parisi, M. A. Rubio, and I. Zúñiga for helpful discussions. Financial support from Grants Nos. PB96-0875 and PB96-0085 (MEC, Spain), and FMRXCT980183 (European Union), is also acknowledged.

APPENDIX

We analyze here the radiation of a crack moving at constant speed in a finite two-dimensional slab in the continuum limit. Let us take the width of the slab as l. The slab is infinite along the x direction, and the boundaries along the y

direction are at $y=\pm l/2$. We look for a solution of the type

$$u_x = f_x(x-vt,y),$$

$$u_y = f_y(x-vt,y), \tag{A1}$$

where v is the velocity of the crack. The normal modes of the slab can be written as

$$a_x = g_x(y)e^{i(\omega_k t-kx)},$$

$$a_y = g_y(y)e^{i(\omega_k t-kx)}. \tag{A2}$$

It is clear that the solution in Eq. (A1) can only include propagating modes, Eq. (A2), when $\omega_k = vk$. In all calculations reported here, $v \leqslant v_R$, where v_R is the Rayleigh velocity. There are no modes at this energy in an infinite slab, $l \to \infty$. In a finite slab, however, we have long-wavelength modes, $k \ll l^{-1}$, which can be emitted by a crack moving at constant velocity. The modes at the lowest energies are such that $g_{x,y}(y) \propto \sinh(\kappa y), \cosh(\kappa y)$. Boundary conditions imply that $\sigma_{xy}(\pm l/2) = \sigma_{yy}(\pm l/2) = 0$. That leads to the following equations:

$$4k^2\kappa_T\kappa_L \tanh\left(\kappa_T \frac{l}{2}\right) = (k^2+\kappa_T^2)^2 \tanh\left(\kappa_L \frac{l}{2}\right),$$

$$4k^2\kappa_T\kappa_L \tanh\left(\kappa_L \frac{l}{2}\right) = (k^2+\kappa_T^2)^2 \tanh\left(\kappa_T \frac{l}{2}\right), \tag{A3}$$

where v_T and v_L are the transverse and longitudinal sound velocities and $\kappa_{T,L}^2 = k^2 - \omega_k^2/v_{T,L}^2$. The solutions correspond to modes either symmetric—Eq. (A4a)—or antisymmetric—Eq. (A4b)—with respect to the slab axis. Finally, other modes at finite energies can be obtained from Eq. (A2) assuming that $g_{x,y}(y) \propto \sin(k'y), \cos(k'y)$. A sketch of the modes of a slab of finite width at low energies is given in Fig. 8.

The Eqs. (A3) lead to the Rayleigh waves at short wavelengths. At very long wavelengths, $k \ll l^{-1}$, one obtains

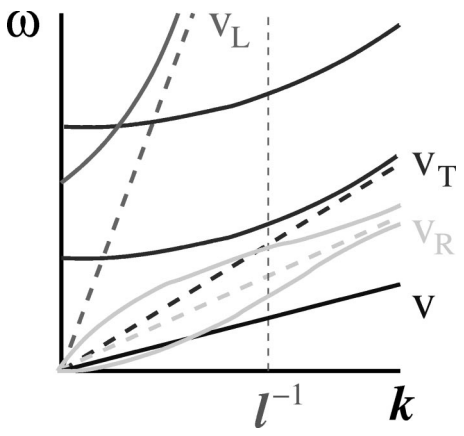

FIG. 8. Sketch of the low energy modes of a slab of width l. The straight line marked v is the line $\omega = vk$. Its intersection with the normal modes marks the frequency of the only mode which can be emitted by the moving crack.

$$\omega_k^s = v_T \frac{2k^2 l}{\sqrt{3}} \sqrt{1-\frac{v_T^2}{v_L^2}}, \tag{A4a}$$

$$\omega_k^a = 2v_T k \sqrt{1-\frac{v_T^2}{v_L^2}}, \tag{A4b}$$

in agreement with general arguments.[41] The only mode that can be associated to the moving crack is ω_k^s in Eqs. (A4a) and (A4b) above. Setting $\omega_k^s = vk$, its wavelength is

$$\lambda_v = \frac{4\pi}{k} = l \frac{2\pi}{\sqrt{3}} \frac{v_T}{v} \sqrt{1-\frac{v_T^2}{v_L^2}}. \tag{A5}$$

Thus, for $v \leqslant v_R < v_T, v_L$, this wavelength is longer than the width of the slab, l. The mode is delocalized in the transverse direction.

In a continuum model, and in the absence of a short-distance cutoff, the mode identified here has null measure. Hence, its influence on the dynamics of the crack is negligible.

[1] L.B. Freund, *Dynamic Fracture Mechanics* (Cambridge University Press, New York, 1990).

[2] J. Fineberg and M. Marder, Phys. Rep. **313**, 1 (1999).

[3] J. Fineberg, S.P. Gross, M. Marder, and H.L. Swinney, Phys. Rev. B **45**, 5146 (1992).

[4] J.F. Boudet, S. Ciliberto, and V. Steinberg, Europhys. Lett. **30**, 337 (1995).

[5] J.F. Boudet, S. Ciliberto, and V. Steinberg, J. Phys. II **6**, 1493 (1996).

[6] E. Sharon, J. Fineberg, and S.P. Gross, Phys. Rev. Lett. **74**, 5096 (1995).

[7] E. Sharon, S.P. Gross, and J. Fineberg, Phys. Rev. Lett. **76**, 2117 (1996).

[8] A. Yuse and M. Sano, Nature (London) **362**, 329 (1993).

[9] E.H. Yoffe, Philos. Mag. **42**, 739 (1951).

[10] L.I. Slepyan, Dokl. Akad. Nauk. **258**, 561 (1981) [Sov. Phys. Dokl. **26**, 538 (1981)]; **37**, 259 (1982).

[11] Sh.A. Kulamekhtova, V.A. Saraikin, and L.I. Slepyan, Mech. Solids **19**, 101 (1984).

[12] M. Marder and S.P. Gross, J. Mech. Phys. Solids **43**, 1 (1995).

[13] D.A. Kessler and H. Levine, Phys. Rev. E **59**, 5154 (1999); D.A. Kessler, *ibid.* **61**, 2348 (2000); D.A. Kessler and H. Levine, *ibid.* **63**, 016118 (2001).

[14] M. Adda-Bedia and M. Ben-Amar, Phys. Rev. Lett. **76**, 1497 (1996); M. Adda-Bedia, R. Arias, M. Ben-Amar, and F. Lund, *ibid.* **82**, 2314 (1999).

[15] E. Louis and F. Guinea, Europhys. Lett. **3**, 871 (1987).

[16] P. Meakin, G. Li, L.M. Sander, E. Louis, and F. Guinea, J. Phys.

A **22**, 1393 (1989); O. Pla, F. Guinea, E. Louis, G. Li, L.M. Sander, H. Yan, and P. Meakin, Phys. Rev. A **42**, 3670 (1990).
[17] O. Pla, F. Guinea, E. Louis, S.V. Ghaisas, and L.M. Sander, Phys. Rev. B **57**, R13981 (1998).
[18] O. Pla, F. Guinea, E. Louis, S.V. Ghaisas, and L.M. Sander, Phys. Rev. B **61**, 11472 (2000).
[19] T. Martín, P. Español, M.A. Rubio, and I. Zúñiga, Phys. Rev. E **61**, 6120 (2000).
[20] F.F. Abraham, Phys. Rev. Lett. **77**, 869 (1996).
[21] S.J. Zhou, D.M. Beazley, P.S. Lomdahl, and B.L. Holian, Phys. Rev. Lett. **78**, 479 (1997).
[22] R.K. Kalia, A. Nakano, A. Omeltchenko, K. Tsuruta, and P. Vashishta, Phys. Rev. Lett. **78**, 2144 (1997).
[23] J.A. Hauch, D. Holland, M.P. Marder, and H.L. Swinney, Phys. Rev. Lett. **82**, 3823 (1999).
[24] I.S. Aranson, V.A. Kalatsky, and V.M. Vinokur, Phys. Rev. Lett. **85**, 118 (2000).
[25] A. Karma, D.A. Kessler, and H. Levine, Phys. Rev. Lett. **87**, 045501 (2001).
[26] Z.P. Bazant and J. Planas, *Fracture and Size Effect in Concrete and Other Quasibrittle Materials* (CRC Press, New York, 1998).
[27] F.J. Gómez Sánchez, Ph.D. thesis, Universidad Politécnica de Madrid, 1998.
[28] J.F. Boudet and S. Ciliberto, Phys. Rev. Lett. **80**, 341 (1998).
[29] J.F. Boudet and S. Ciliberto, Physica D **142**, 317 (2000).
[30] E. Sharon, G. Cohen, and J. Fineberg, Nature (London) **410**, 68 (2001).
[31] R.C. Ball and A. Parisi (unpublished).
[32] E. Bouchaud, J.-P. Bouchaud, D.S. Fisher, S. Ramananthan, and J.R. Rice, cond-mat/0108261 (unpublished).
[33] K.N.G. Fuller, P.G. Fox, and J.E. Field, Proc. R. Soc. London, Ser. A **341**, 537 (1975).
[34] L.M. Sander and S.V. Ghaisas, Phys. Rev. Lett. **83**, 1994 (1999).
[35] L.B. Freund, J. Mech. Phys. Solids **20**, 129 (1972); **20**, 141 (1972).
[36] J.R. Willis and A.B. Movchan, J. Mech. Phys. Solids **43**, 319 (1995).
[37] H. Larralde and R.C. Ball, Europhys. Lett. **30**, 287 (1995).
[38] S. Ramanathan and D.S. Fisher, Phys. Rev. Lett. **79**, 877 (1997).
[39] J.M. Morrissey and J.R. Rice, J. Mech. Phys. Solids **46**, 467 (1998).
[40] J.M. Morrissey and J.R. Rice, J. Mech. Phys. Solids **48**, 1229 (2000).
[41] L. Landau and E. Lifshitz, *Theory of Elasticity* (Addison-Wesley, Reading, MA, 1959).
[42] D.A. Kessler and H. Levine, Phys. Rev. E **60**, 7569 (1999).